Urbanizational impact on climatic variables and geographical analysis of physical land use land cover variation of a city using Remote Sensing.

Santhana Iyyappa Sundararaj S[1], Dr. Chandramathy I[2], Dr.Jeykumar R.K.C[3], Dr. Chandramohan K[4],

[1*]Associate Professor, Department of Civil Engineering, Sethu Institute of Technology, Virudhunagar Email ID: pothiarch83@gmail.com
[2]Professor, Department of Architecture, Thiagarajar College of Engineering, Thirupparankundram, Madurai-625009, Tamil Nadu, India. E-mail ID:cmarch@tce.edu
[3]Assistant Professor, Department of Civil Engineering, Thiagarajar College of Engineering, Thirupparankundram, Madurai-625009, Tamil Nadu, India. E-mail ID: rkcjey@gmail.com, cell: +919150077046.
[4]Dr.Chandramohan K, Lecturer, Department of Environmental Remote Sensing and Cartograpy, Madurai Kamaraj University, Madurai.
[*]Corresponding author:Ar.Santhana Iyyappa Sundararaj S,
E.mail:pothiarch83@gmail.com, tel:+91 04566 229700

Graphical abstract

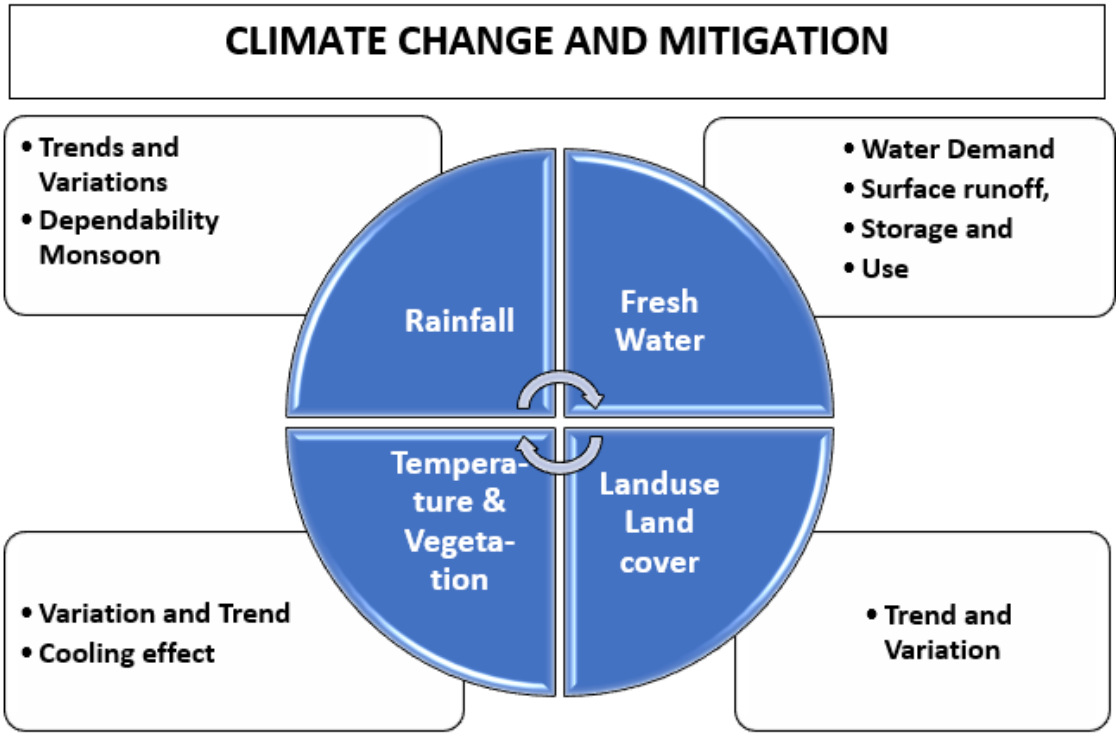

Abstract

Climate change has serious implications for the rise and variation of the average earth's temperature and intensified rainfall. In urban areas, temperatures and intensified rainfall variation are noticeably seenin the city which disrupts the normal life of living things. Also, it affects the storage of rainfall

runoff water in tanks and lakes. Green cover reduction due to the increase ofagriculture, industrialization, population explosion and urbanization have a direct impact on the climate pattern.The average temperature of a city is increasing every decade due to a drastic reduction in the green cover.This is visible today from the abnormal melting of glaciers. The rainfall pattern is highly intensified, and the frequency of rainfall is on a decreasing trend. This intensified rainfall creates high surface runoff during rainfall and disrupts the normal life in a city.

The Standard Precipitation Index (SPI) for a city indicates a noticeable shift in its climatic pattern, particularly with consistent rainfall during the southwest monsoon. Over the span of four decades, LULC research has revealed an increase in residential areas and a decrease in green cover. This urbanization process is associated with changes in LULC, resulting in decreased vegetation and diminished storage water bodies.Variations in the temperature of city are on an increasing trend. Urban forestry or the dense green coverof an area reduces the temperature and creates cool pockets in the city. The regression model for temperature and vegetation indicates the negative correlation of temperature with high vegetation growth.

Keywords: Urbanization, Climate change, Rainfall-runoff, Temperature, Green Cover

1.Introduction

1.1 Background

Global warming and climate change are serious threats to life on Earth. The rise of temperature in a city creates a temperature heat wave, and results in the loss of human life. Dwindling freshwater resources challenge the policymakers to meet the needs of all living things for their day-to-day biological process, and become a rising concern in any city. The demand for freshwater resources is increasing in the agriculture sector , industrial sector, Domestic sector. Today, the consumption of Fresh Water has more than tripled globally since 1950. Around 1.2 billion individuals annually face challenges in accessing safe water supply and sanitation, constituting approximately one-sixth of the global population, as per the reports of the World Health

Organization (WHO) and UNICEF in 2000. The most recent Global Environment Outlook from the United Nations Environmental Programme (UNEP) reveals that around one-third of the world's population lives in countries with moderate to high water stress, where water consumption surpasses 10% of renewable freshwater resources. According to the United Nations Environmental Programme (UNEP) most recent Global Environment Outlook, almost one-third of the world's population lives in countries with moderate to severe water stress, when water demand exceeds 10% of renewable freshwater resources. Effective management of urban rainfall runoff water requires a scientific understanding of how human activities impact the urban hydrological cycle and the environment. Temperature fluctuations are a significant concern, leading to increased risks to human life. Urban green cover or forestry plays a vital role in cooling and mitigating heatwaves. Anthropogenic influences vary significantly across different time periods and geographical locations, requiring measurements that consider urban expansion, local climate, cultural norms, environmental factors, religious beliefs, and socio-economic factors. (Jiri Marsaleket al.,2007).

The Fourth Assessment Report of the the Intergovernmental Panel on Climate Change (IPCC, 2007) highlighted a global trend towards increased susceptibility to drought, marked by more frequent extreme events. This pattern can be seen in a variety of regions around the world, including changes in monsoonal rainfall in India due to climate change (Naidu et al., 2009), increased occurrences of drought in the United Kingdom (Arnell, 2007), and the Indian subcontinent (Sivakumar and Stefanski, 2011), emphasising the effects of climate change (Mundetia N and Sharma D, 2015). The mean surface temperature across India aligns with the documented increase in global surface temperature, as supported by Pant et al. (1999), Singh et al. (2001), Krishnan et al. (2016), Lairenjam C. (2017), and Dash et al. (2019). Shastri et al. (2017) similarly noted a rising trend in surface temperatures across various Indian regions.

Climate change leads to increased runoff even in regions with abundant rainfall and snowfall (Sarkar, 2015), while simultaneously decreasing infiltration, thereby reducing aquifer recharge. Regional variations in temperature and rainfall disrupt the hydrological cycle, posing a significant

threat to global freshwater resources (Sarkar A, 2015). Pollution due to anthropogenic sources with various demands for fresh water such as domestic application and industrial application, as well as non-point sources discharges wastewater on the land which have a negative impact on fresh water quality. Groundwater supplies in places where surface water is harvested can become contaminated as a result of poor sanitary infrastructure. Consequently, there is an urgent necessity to manage freshwater resources, including the quality and quantity of runoff rainfall, and effectively conserve runoff for both current and future urban needs.

Withanage, W. K. N. C. et al., reported that the builtup area is on the increasing trend and coconut farming is on the decreasing trend. Kevin S. Sambieni,et.al., reported that settlement, water bodies and agricultural areas are on the increasing trend whereas wooded land, Forest and Savanna are on the decreasing trend. Land surface temperature is known to be related to LULC types (Chen et al., 2006; Connors et al., 2013; Weng, 2001; Xian and Crane, 2006), and there exists the relationship between the spatial structure of urban thermal patterns and urban surface characteristics (Li et al., 2011; Liu and Weng, 2008; Weng et al., 2007).

1.2 Study area

Madurai is one of the heritage cities in Tamilnadu, India located within latitudes 9°56′N to 9.93°N and longitudes 78°07′E to 78.12°E and has an average elevation of 101 meters above mean sea level. Madurai is located on the banks of the River Vaigai which is the resource for fresh water for the residents of Madurai for two millennia and is one of the oldest city in the world which is continuously inhabited settlements. The city has a very rich architectural heritage and ecological heritage. The city is referred to as the cultural capital of Tamilnadu, India. Madurai is also referred to as “Kadambavanam” which is the Land composed of the Forest of Kadamba Trees. Madurai is an important city in the state of Tamilnadu.

Madurai City is the second largest corporation city by area and has expanded to 100 wards recently having the third largest population Tamil Nadu. The city area spreads to an extent of 148

km^2. The population of the city was 15,73,616 numbers in the year 2017. The population density is increased from 733 persons/sq km in 1990 to 823 persons/sq km in 2011 and has undergone a drastic transformation with developments in Physical and Social Infrastructure across the years. The location and map of Madurai corporation are shown in Figures 1 and 2, given below.

Figure 1 Location of Study Area

Figure 2 Map of Madurai corporation**Meteorology**

Madurai has a semi-arid tropical climate with temperature ranges between 40°C and 26.3°C in summer and 29.6°C and 18°C in winter. Madurai experiences an average temperatures ranging from 20.3°C to 37.7°C, with the peak heat reaching in May at37.7°C. The minimum temperatures are recorded in December and January, with the mercury dropping to 20.3°C and 21.5°C, respectively.

Annual average rainfall of the city is about 850 mm with an average humidity is 65%. Monthly rainfall in Madurai varies from 6mm to 120mm, with October being the wettest month at 120mm. The lowest monthly rainfall occurred in January, registering a mere 6mm. The city experiences an average of around 5 to 23 rainy days a month with the maximum number of wet days in October. The relative atmospheric humidity lies between 51% and 75%, with December and January being the most humid months.

2.Methods and Techniques

2.1 Objectives of the study

The objectives are

a. To investigate the influence of urbanisation on Madurai's rainfall and temperature patterns

b. To investigate the physico-geographical variance through land use and land cover analysis with Remote Sensing and Geographical Information Systems.

c. To analyze the mitigation measures of urbanization impact to control micro-climate.

2.2Data Collection and Synthesis

Secondary data, including population census data, rainfall records, temperature data, and Landsat study area RS-GIS images. have been gathered. The rainfall data of a city comes from the State Groundwater Resources Data Centre of Tamil Nadu. The collected information undergoes analysis for essential hydrological characterization, encompassing rainfall trends, runoff, population growth, groundwater recharge, and land-use/land-cover patterns. Population data is sourced from the Census Department's website. GIS images for the years 1990, 2000, 2010, and 2020 are acquired from the USGS website and processed using Arc-GIS to assess urbanization extent and variation in land-use/land-cover patterns. GIS images are acquired from LANDSAT 8 satellite having 30m resolution with 1 in 25000 scale. from Statistical rainfall analysis entails descriptive statistics, regression analysis, probabilityprobability analysis observed and predicted (P-P), correlation absolute within the months, and the production of P-P plots, Box plots, Area plots, and other graphical representations.The temperature data of a city is obtained from the State Government Department for analysis. DrinCa free software developed by the National Technical University of Athens is used to analyze the standard precipitation index (SPI).

Also, in this study, the impact of dominant urban green cover abutting the urban residential neighborhoods is assessed using remote sensing images. The urban area was digitized using Google Earth Imagery and the area of the green cover is computed using ArcGIS. Field investigation is also conducted to findout the reality of the land use and land cover existing in the urban area. Multiple buffer zones are created at 50m intervals around the urban greenery using ArcGIS to assess the temperature variation. The maximum limit of the buffer region chosen for the temperature variation study is 500m. Land surface temperature is analyzed using Remote Sensing image data through radiance, brightness, and land surface emissivity. The Standard Vegetation Index analysis procedure and the procedure followed to extract temperature data from remote sensing images are given below.

2.2.1 Standard Vegetation Index Analysis

Standardized Vegetation Index is calculated from the Normalized Difference Vegetation Index (NDVI) using Near Infra-red (Band 5) and Red (Band 4) bands as given below.

$$NSVI = (NIR - RED)/(NIR + RED)$$

Where:

NSVI = Normalised Standard Vegetation Index

RED = Digital numbers (DN) Values from the RED Band

NIR = Digital numbers (DN) Values from Near Infra-red Band

2.2.2. Radiance Analysis:

In radiance image analysis, Thermal Infra-Red Digital Numbers are converted to spectral radiance to find out atmospheric brightness using spectral radiance through the rescaling factor. A spectral radiance is obtained using the formula given below.

$$L\lambda = ML * Q_{cal} + AL - O_i$$

$$L\lambda = 0.0003342 * Band10 + 0.10000 - 0.29$$

Where:

$L\lambda = TOA$ (Top Of Atmosphere) spectral radiance (Watts/$(m^2 * sr * \mu m)$)

ML = Radiance multiplicative Band (No.)

AL = Radiance Add Band (No.)

Q_{cal} = Quantized and calibrated standard product pixel value (DN)

O_i = correction value for band 10 is 0.29

2.2.3 Atmospheric Brightness Analysis

The brightness in the atmosphere is directly related to the temperature and hence, Spectral radiance data can be converted to temperature using the thermal constant values in the Meta data file as given below.

$$BT = K2 / \ln(K1 / L\lambda + 1) - 273.15$$

$$BT = (1321.0789 / Ln(774.8853 / TOA + 1)) - 273.15$$

Where:

BT = Top of atmosphere brightness temperature (°C)

$L\lambda = TOA$ spectral radiance (Watts/$(m^2 * sr * \mu m)$)

K1=Constant Band (No.)

K2=Constant Band (No.)

2.2.4 Land Surface Emissivity (LSE) analysis:

Land Surface Emissivity (LSE) is the average emissivity of an element of the surface of the earth can be calculated from NDVI values as given below

$$PV = ((NDVI - NDVI_{min})/(NDVI_{max} - NDVI_{min}))^2$$

Where:

PV = Proportion of Vegetation

NDVI = DN Values from NDVI Image

$NDVI_{Min}$ = Minimum DN Values from NDVI Image

$NDVI_{Max}$= DN Values from NDVI Image

$$E = 0.004 * PV + 0.986$$

Where:

E = Land Surface Emissivity

PV = Proportion of Vegetation

0.986 corresponds to a correction factor value of the equation

2.2.5 Land Surface Temperature Analysis

Land Surface Temperature (LST) is the radioactive temperature, calculated using atmosphere brightness temperature, Wavelength of emitted radiance, and Land Surface Emissivity as given below.

$$LST = BT/\left(1+\left(\lambda * BT/c^2\right)*\ln(E)\right)$$

Here, c^2 = 14388 μm K

The Values of λ for Landsat 8: For Band 10 is 10.8 and for Band 11 is 12.0

Where:

BT = Top of atmosphere brightness temperature (°C)

ʎ = Wavelength of emitted radiance

E = Land Surface Emissivity

$$C2 = h*c/s = 1.4388*10^{-2}\,mK = 14388\mu mK$$

H = Planck`s Constant = $6.626*10^{-34}$ J s

S = Boltzmann Constant = $1.38*10^{-23}$ JKs

C = Velocity of Light = $2.998*10^{8}$ m/s

3.Results and Discussion

The analysis is being undertaken for Landuse Landcover (LULC) to better understand patterns in city expansion and changes in land use areas, with the goal of managing both surface and groundwater resources. Rainfall-runoff analysis is performed to better understand the trend of rainfall-runoff patterns and to manage freshwater resources more effectively.

3.1 Population growth and LULC analysis

The population of Madurai cityis 10.18 lakhs in the year 2011. At present, the population is 14.65 lakhs approximately in the year 2023 as obtained from the census. The sudden jump of 40% is due to the creation of 28 more wards that are annexed in the extension area of Madurai Corporation. The linear forecast population growth curve of the city shows the expected population of 1630000, 1900000 and 2250000 in the years 2031, 2041, and 2051respectively which is shown in the figure 3 given below. The buildup area increase of 29.94% from the year 2010 to 2020, is similar to the increase in the population percentage increase of 9.4%. The increase in the percentage of buildup area nearly three times as population percentage shows that the development of the city is horizontal.Landuse Landcover for four decades are shown in table 1below. As the corporation area limit increases, buildup area alsoincreases which has a direct correlation to the population of Madurai. Landuse Land cover analysis may be used to estimate the year wise population as the growth of buildup area is horizontal.

Table 1 Landuse Landcover Analysis

Figure 3 Population Growth curve

Figure 4 identifies various apportion of LULC areas in Madurai for the year 1990, 2000, 2010, and 2020 with linear forecast trend line of LULC. This trendline, forecast the apportionment of the use of the city's LULC for the year 2040. The linear forecast trend line for the year 2040 predicts that the sparse vegetation is almost nil and dense vegetation is reduced to 15%. High density buildup increases to 22%, medium density buildup increases to 31% and low density buildup increases to 23%.

Figure 4 Landuse Landcover variation from 1990 to 2020 and future linear trend line till 2040

3.2 Land use Land cover analysis (LULC)

The LULC analysis is made to identify various land cover areas, especially Vegetation, Buildup areas, Water spread areas, Sand and Rocky areas, Unvegetated and Barren land, etc.

3.2.1 Land use and land cover for the year 1990

The LULC analysed for the year 1990 identifies the percentage of dense vegetation as 42.42%, less dense vegetation as 27.74%, the residential high density buildup as 6.14%, medium density buidup as 8.84% and low density buildup as 4.79%, the sandy area as 0.22% and the rocky area as 1.13%, the area of water spread as 1.35%, and the barren land as 6.98%. The digitized image of the Landsat image for the year 1990 is shown in Figure 5.

Figure 5 Landuse and Landcover for the year1990

3.2.2Land use and land cover for the year 2000

The LULC analysed for the year 2000 identifies the percentage of dense vegetation as 35.32%, less dense vegetation as 30.48%, the residential high density buildup as 7.85%, medium density buidup as 10.32% and low density buildup as 5.28%, the sandy area as 0.24% and the rocky area as 1.16%, the area of water spread area as 0.83%, and the barren land as 8.14%. The digitized Landsat image for the year 2000 is shown in Figure 6.

Figure 6 Landuse and Landcover for the year2000**3.2.3Land use and land cover for the year 2010**

The LULC analysed for the year 2010 identifies the percentage of dense vegetation as 31.36%, less dense vegetation as 19.94%, the residential high density buildup as 12.72%, medium density buidup as 17.07% and low density buildup as 10.15%, the sandy area as 0.46% and the rocky area as 0.96%, the area of water spread area as 2.42%, and the barren land as 4.46%. The digitized image of the landsat image for the year 2010 is shown in Figure 7.

Figure 7 Landuse and Landcover for the year2010

3.2.4 Land use and land cover for the year 2020

LULC analysed for the year 2010 identifies that the percentage of dense vegetation as 25.76%, less dense vegetation as 11.09%, the residential high density buildup as 15.42%, medium density buidup as 21.86% and low density buildup as 16.36%, the sandy area as 0.65% and the rocky area as 0.96%, the area of water spread area as 2.42%, and the barren land as 3.18%. The digitized landsat image for the year 2020 is shown in Figure 8.

Figure 8 Landuse and Landcover for the year2020

LULC images of Madurai for the years 1990, 2000, 2010 and 2020 are showing a decline pattern in urban green cover due to urbanisation as shown in Figure 4. The LULC pattern of 2020 from 1990 shows the dense vegetation area as reduced by 16.66and less dense vegetation by 16.65%. This LULC analysis also shows there is an increase in high build up by 9.28% , mediumdensity buildup by 13.02%, and low density buildup by 11.57%. This clearly indicates that the population of the city is on a growing trend. The low density buildup transforms to medium density buildup, medium density buildup to high density buildup respectively.The LULC pattern reflects that the residential builtup area development is haphazard and develops at an abnormal rate. The water spread area varies depending on the monsoon of the year and it shows that the rainfall is intensified.

3.3Rainfall and Runoff analysis

Statistical analysis of rainfall includes descriptive statistics, regression analysis, probability-probability analysis for observed and predicted (P-P), absolute correlation among months, and the creation of graphical representations such as P-P plots, Box plots, Area plots, and others. Descriptive statistics for monthly rainfall spanning from 1991 to 2011 are presented in Table 2. The average annual rainfall (AAR) in Madurai city is recorded at 850mm, with a standard deviation of 86mm, equivalent to 10.1% of the AAR. The maximum annual rainfall reaches 1007mm, marking an 18.5% increase from the average, while the minimum recorded rainfall is 709mm, indicating a 16.6% decrease from the average. Surpluses in average annual rainfall are notably contributed by September, October, November, and December.

Table 2 Descriptive statistics of monthly Rainfall from 1991 to 2021

The annual rainfall with a linear trend linefor the years 1991 to 2021 is shown in Figure 9 and this trendline analysis identifiesthat the annual rainfall of the city has above AAR from the year 2002 to 2013. From the year 2014 onwards the rainfall started oscillating from too low and slightly above average. The linear trend of the rainfall shows a dip towards below average rainfallfrom above

average rainfall for the years 1990 to 2021. The rainfall generally shows a declining trend from 1991 to 2021. Also, a chart is drawn showing the yearly rainfall of a month from 1991-2021 is shown in Figure 10. It is seen from the figure that the rainfall is on the increasing trend in July and on the decreasing trend in August. This indicates that there is a shift of rainfall from August to July. Also, it is seen that the rainfall shift starts from June to September. This indicates that the monsoon sets early. The pie chart in Fig 11 illustrates the monthly average rainfall distribution from 1991 to 2021, indicating that the city receives the majority of its average annual rainfall during June, July, August, followed by September. Skewness and Kurtosis coefficients are lower during July and August, indicating minimal deviation from normal monthly rainfall, as depicted in Table 2. Figures 12, 13, 14 and 15 display yearly rainfall trends from January to December, with an increasing trend observed in January, May, June, July, and November, and a declining trend observed in February, March, August, September, October, and December. The Normal Observed Probability Vs Expected Probability (P-P) plots for July and August in Figures 16 and 18 show the least deviation from the 45-degree line. The range of deviation for these months, as indicated by the detrended normal P-P plots in Figures 17 and 19, varies from +0.1 to -0.075 for July and +0.075 to -0.075 for August. These months are crucial for effective planning of water resources for domestic use

Figure 9 Annual rainfall and Trend line from 1991 to 2021

Figure 10Yearly rainfall of a month from 1991-2021

Figure 11Average monthly rainfall

Figure 12 Yearly rainfall and Trend line for months Jan-Mar

Figure 13 Yearly rainfall and Trend line for months Apr-Jun

Figure 14 Yearly rainfall and Trend Line for months July-Sep

Figure 15 Yearly rainfall and Trend line for Oct-Dec

Figure 16 P-PNormal chart for July month

Figure 17 Detrended normal P-P chart for July month

Figure 18 P-PNormal chart for August month

Figure 19 Detrended P-P chart for August month

Table 3 Proximity matrix – Absolute rainfall correlation for months and annual rainfall

The correlation matrix as given in the Table 3 is a proximity matrix and the correalation between months are insignificant. A significant correlation occurs between AAR in July and August which is 0.55 and 0.45. These months provide more than 40% of the average annual rainfall.Nearly 60% to 65% of the rainfall is obtained in the months from June to September. These months are highly effective in planning water resources for domestic uses.

Figure 20 Box plot for monthly rainfall Vs year of rainfall

The box plot of monthly rainfall Vs year of rainfall which is shown in Figure 20. This plot identifies that there is a large variation in the monthly rainfall from June to September i.e. south west monsoon but not abnormal. The abnormal yearly positive variations are found in the year 1992 for the month of March, Year 2005 for the month of January, the Year 2007 for the month of October, and the Year 2021 for the month of November. The abnormal negative variation is found in the year 1999 for the month of May. South-west monsoon is highly effective in planning water resources for domestic uses.

P-P plot, correlation, and box plot show greater significance in July and August months rainfall and hence the surface runoff of these monthsis to be conserved and shall be used in the city for domestic uses. In general, south-west monsoon rainfall shall be taken for planning for fresh Water resources management of the city since it is highly reliable. It is also to be noted that the rainfall is not of uniform frequency throughout these months but the rainfall is intensified with less frequency of rainfall. A proper careful planning is necessary to harvest surface runoff with intensified rainfall.

3.4 Regression analysis

Table 4 presents the results of the linear regression correlation analysis conducted on monthly rainfall data against the Annual Average Rainfall (AAR). Monthly rainfall serves as an independent

variable and the average annual rainfall acts as the dependent variable. The standardized beta coefficients for July, August, September, and June are 0.72, 0.79, 0.38, and 0.37 respectively. This analysis reveals that rainfall in July and August exerts the greatest influence on AAR, followed by September and June. It also indicates that these months contribute the majority of rainfall annually, highlighting the reliability of the south-west monsoon for freshwater resource management.

Table 4 Regression correlation between Monthly rainfall and Annual Rainfall

3.5 Water Demand Analysis

In terms of water demand analysis, Madurai city's population stands at 14,65,625 as of 2023. According to the Central Public Health Environmental Engineering Organisation (CPHEEO), a Central Government organization in India, the minimum per capita domestic water provision should be 135 liters per capita per day (lpcd). Based on this recommendation, Madurai City requires an annual supply of 72 Mm^3 of water. Madurai is an ancient city renowned for its architecture and foresight in harnessing natural resources. It boasts a network of built-in natural storage structures known as tanks, designed by ancestors to store surface runoff and surplus water from the Vaigai River. These tanks are interconnected, allowing overflow from upstream tanks to fill downstream ones until the series culminates in the river. This system not only stores freshwater but also serves as flood control. However, the haphazard urban development has led to the loss of channels and disrupted the hydraulic flow within the tank series.

3.6.1Surface runoff analysis

Regression analysis proves that the south-west monsoon provides a maximum rainfall Surface runoff is being estimated for this monsoon by using the United States Department of Agriculture Soil Conservation Service Curve Number technique. The rainfall during the south -

west monsoon provides nearly 60% of the rainfall and it is 510mm. The surface runoff during the period in the city is 74Mm^3. Nearly 25% of this water is lost due to evaporation and infiltration. The balance of fresh water that can be stored in the south- west monsoon will be 55.5 Mm^3 with proper planning and management of surface runoff. This stored surface runoff will cater to the Madurai population for nine months. But as of now the domestic needs of water is taken from Vaigai Dam. It is highly necessary and essential to create local source of freshwater sources in the city which reduces cost of transportation of water and also the cost of infrastructure. The estimation of surface runoffprovided above is for the area within the Madurai Corporation limits. In future, it may be planned to preserve surface runoff in the entire district of Madurai. As of now the surface runoff is either infiltrated or evaporated. The existing tanks and channels may be modernized to store surface runoff and surplus water may be drained into river Vaigai of the city.

3.7 Standardized Precipitation Index (SPI)

The SPI chart for Madurai city, as depicted in Figure 21 of the study conducted by Nasrin Salehnia et al. in 2017, illustrates yearly rainfall patterns and is utilized to determine normal, wet, and dry conditions. It indicates an extreme wet condition (value >2) occurring in the year 2007-08. The SPI ranges from 1.5 to -1.75 between 1991 and 2021, except for 2007-08, indicating near-normal to severe dry conditions during that period. Since 2000-2001 to 2018-2019, the SPI has been nearly normal (-0.99 to 0.99), except for 2007-2008, highlighting an extremely wet condition solely in that year. This fluctuation in SPI suggests a change in climate patterns, with the yearly linear trend line indicating a shift from wet to dry conditions. Additionally, SPI is analyzed for monthly variations from 1991 to 2021 and categorized accordingly, as demonstrated in figures 23 to 26.. The monthly SPI index linear trend line shows that the February, March, April, August, September and October changes from wet to dry condition. The trend line for the month of January, May, June and July show the changes from dry to wet condition.

Figure 21 Yearly SPI index

Figure 22Monthly SPI index for January to March.

Figure 23MonthlySPI index for April to June.

Figure 24MonthlySPI index for July to September.

Figure 25 Monthly SPI index for October to December.

3.8 Temperature Analysis

Climate change mainly focuses on the average temperature of the earth. Temperature analysis is done for the monthly obtained data for Average, Maximum, and Minimum values during the years 1991-2021 of the cityand is shown in Figure 26. Temperature average shows the variation of 0.5^{o} C to 0.75^{o}C, the temperature minimum shows the variation of 1.5^{o}C to 2^{o}C, and the temperatue maximum shows a variation of around 3^{o}C from the year 2019. Maximum, and Minimum Temperature figure show that there is a decline in the temperature of the city since 2018. This indicates that the number of cyclones and variations in the sea environment are greater from 2018 compared to previous years, thus resulting in the temperature dip as shown in Figure 27. This indicates there is a climate change in global phenomenon that affects the city as well. This wide variation may be the effect of the alarming increase in the melting of snow cover.

Figure 26 Temperature Maximum, Average and Minimum

3.8.1 Land Surface Temperature variation within the city

Land surface temperature is extracted from Landsat images by analysing atmospheric brightness, radiance wavelength, and land surface emissivity.Thermal infra-red data obtained is converted to spectral radiance. This spectral radiance is then converted to atmospheric brightness. Land surface emissivity is then obtained from the proportion of vegetation. Finally, Land surface temperature is obtained from atmospheric brightness and Land surface emissivity. Land surface temperature is shown in Figure 27.

Figure 27 Temperature variation of the city

3.8.2. Temperature variation due to Urban Green cover

Temperature of the earth is directly related to the vegetation cover. The decrease in vegetation cover reduces the water retention capacity of the soil surface, while an increase in infrastructure leads to a further decrease in vegetation cover. Also, vegetation cover is not evenly spread, but it has small dense pockets within the city. Landsat images are used to extract the vegetation cover and also the temperature prevailing in the dense vegetation-covered and adjoining areas of the city. The Standard vegetation index is used to demarcate the vegetation cover.

Madurai city has a greater percentage of the green cover located in the southwestern part of urban Madurai with woodlands abutting to the residential neighbourhood. Southern Railway Residential Colony (SRRC) with dominant dense green spaces is identified for this study which consists of green cover in the form of woodlands and adjoining areas such as Soma Sundaram Residential Colony (SSRC), Ellis Nagar Residential Colony (ENRC) and Agrini Residential Enclave & Colony (AREC) are takenup to analyse variation in temperature as shown in Figure 28 (google imagery) and Figure 29(NDVI of the study area). The difference in temperature is analysed by field visits too.

Figure 28 Google images of urban forestry and adjoining areas

Spatial distribution of standard vegetation index in the study area is shown in Figure 29. The standard vegetation index in the woodlands of Southern Railway Residential Colony (SRRC) ranges from 0.23 to 0.31 and in the adjoining areas of Soma Sundaram Residential Colony (SSRC), Ellis Nagar Residential Colony (ENRC) and Agrini Residential Enclave & Colony (AREC) ranges between -0.11 to 0.19.

Figure 29 NDVI of areas of SRRC with adjoining areas

The Spatial distribution of standard temperature in the study area is shown in figure 30. Temperature in the woodlands of Southern Railway Residential Colony (SRRC) is 26 degrees Celsius and in the adjoining areas of Soma Sundaram Residential Colony (SSRC), Ellis Nagar Residential Colony (ENRC) and Agrini Residential Enclave & Colony (AREC) varies between 26

degree celsius to 31 degrees Celsius.Temperature gradually increases from the core of the green spaces of the woodlands in Southern Railway Residential Colony towards the periphery of the buffer region. Surface temperature measures 26 degrees Celsius in small green space located at 250m from the boundary of the woodlands. Similarly, the surface temperature measures 26 degrees Celsius in small green spaces and spaces with urban trees located outside the buffer region of 500m. Spatial distribution of the Standard Vegetation Index and Temperature of a city are shown in Figures 29 and 30 respectively

Figure 30 Standard Vegetation Index of the city

This study shows that the presence of green cover such as a single tree, group of trees in open spaces, or row of trees in urban residential neighborhoods exhibits less surface temperature than the nearby surrounding areas, which are generally referred to as Urban Cool Islands or pockets. The extracted temperature shows that the green cover region or urban forestry reduces temperature and shall be planned in cities to resist heat waves. These greeneries provide moisture through evapotranspiration and hence the green cover helps to reduce the temperature or create Urban Cool Islands.

4.CONCLUSION

The rainfall pattern in Madurai district is found to be non-uniform or intensified with less frequency of rainfall. This intensified rainfall creates more runoff and proper planning and management are to utilize these freshwater resources effectively. Annual Rainfall from the year 1991 to 2021 moves around 850mmand the trend line shows the rainfall from 1991 to 2014 has rainfall above or equivalent to 850mm and after 2014 onwards the rain falls below 850mm. The Standard deviation of rainfall is around 17% to 18%. Nearly 65% of the rainfall is received in the months of June to September which is due to south-west monsoon.The box plot shows that there is a large variation in the monthly rainfall during the month of June, July, August and September.These months bring rainfall with the onset of south west monsoon. The standardized beta coefficient of

regression analysis identifies that the rainfall in the month of July and August is the most influencing AAR followed by June and September. There is a shift of increase in rainfall in the month of July and August. The increase or decrease in the AAR of a year, reflects predominantly in the months of July and August. P-P analysis plot identifies that the rainfall in these months is consistent. The Skewness and Kurtosis coefficient is also less during the month of June to September which is identified from the minimum deviation of normal monthly rainfal.The total surface runoff available for the city is 72 Mm^3 per year. The average south-west monsoon provides a runoff water of 55Mm^3 per year which is sufficient to cater to the domestic water need for nine months. The land use land cover analysed pattern identifies that the city builtup residential area development is haphazard and develops at an abnormal rate. The dense and sparse vegetation cover is on the decreasing trend and the buildup area is on the increasing trend. LULC pattern depicts Linear ribbon growth development or the development is horizontal in Madurai city. Sustainability needs sustainable planning of fresh water resources from surface runoff and management to protect and create the surface water bodies. Recharge of ground water is equally important to improve the water table with excess runoff. This recherché structure shall be the abandoned wells in a city or desilting of Channels, ponds and tanks which may increase the storage of rainfall runoff. Surface runoff of a city shall be discharged to the recharge pit along the geological fault or fracture area after catch pit. The geological fault or fracture shall be identified along the storm water drain and is discharged. Remote Sensing and Geographical Information Systems (RS-GIS) are a handy tool which may be used effectively to forecast population from buildup areas, and to evaluate the loss of vegetation due to urban expansion.

The presence of green cover in residential neighbourhood reduces the land surface temperature and improves the better outdoor thermal environment. In urban areas, especially the NDVI ranges from – 0.15 to – 0.11 are highly suitable for planting the trees to improve the urban cooling effects as well as mitigating air pollution thereby global warming, because these areas are having sufficient space for planting trees. Planting trees or urban greeneries may be envisaged in any form such as a single urban tree, row of urban trees along the streets, roads, in the parks and

playgrounds, andcreation of urban forests in unvegetated Government lands within the urban areas. These mitigation provides a reduced thermal environment in urban residential neighbourhoods.These urban green cover reduces the heat by 2 to 3 Degrees in the surrounding areas which creates a Urban cool packets or islands. The urban green cover also reduces the carbon-di-oxide in the ambient air and air pollution.Effective planning and design of urban green spaces in the residential neighbourhood helps to minimize the surface land temperature, air pollution and exhibits a strong urban cool island effect or reduced temperature effect.

Acknowledgement

We thank our Management and the Principal of Thiagarajar College of Engineering, Madurai, for encouraging in research activities and also providing us with all the resource facilities for deepening our knowledge through library, e-resources, journals, software and internet required for conductingthis research work successfully. We thankthe Department of United States Geological Survey for distributing the RS images which are very useful for this study. Wethankthe State Groundwater Resource Department of Public Works Department for providing the relevant data to complete this work.We also thank National Technical University of Athens for distributing the free software DrinCwhich is used in this study to find standard precipitation index. We thankall the people for their valuable suggestions and comments during the course of the work. We thankall the authors referred herein and to the authors contributing similar nature of the work to the world forthe effective management of fresh-water resources. Finally, we thank all the peer reviewers for their fruitful comments to enhance the quality of this paper.

Figure 1 Location of Study Area

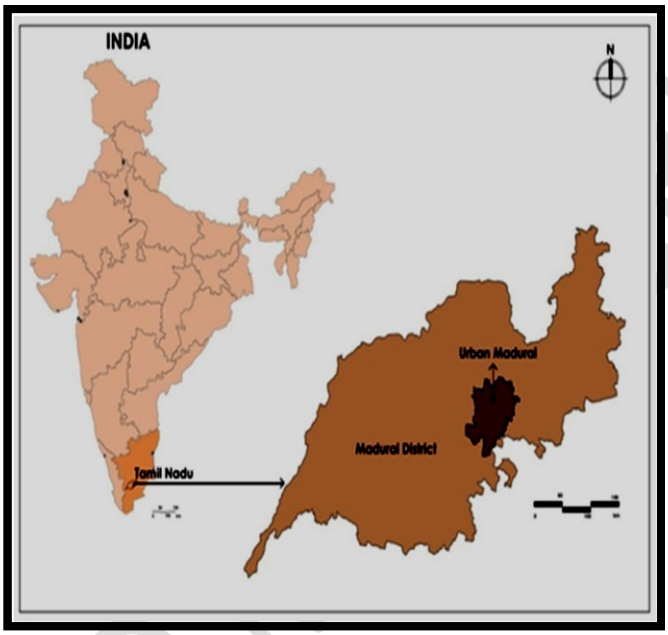

Figure 2 Map of Madurai Corporation Boundary

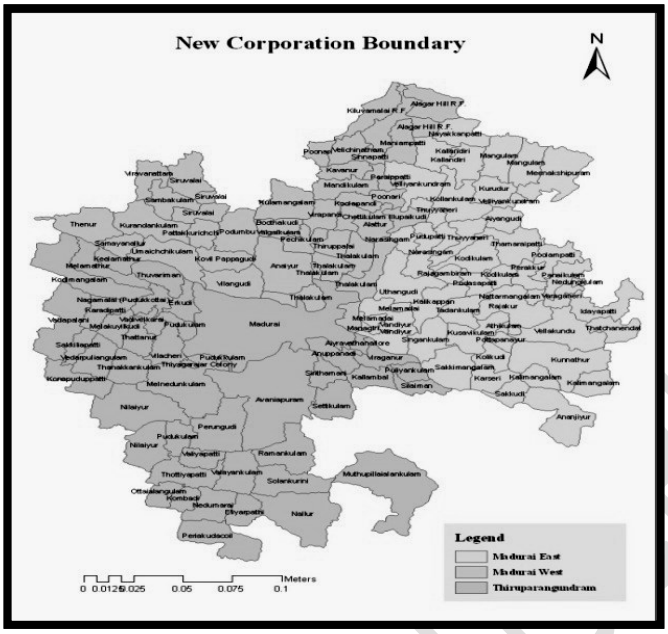

Figure 3 Population Growth Curve

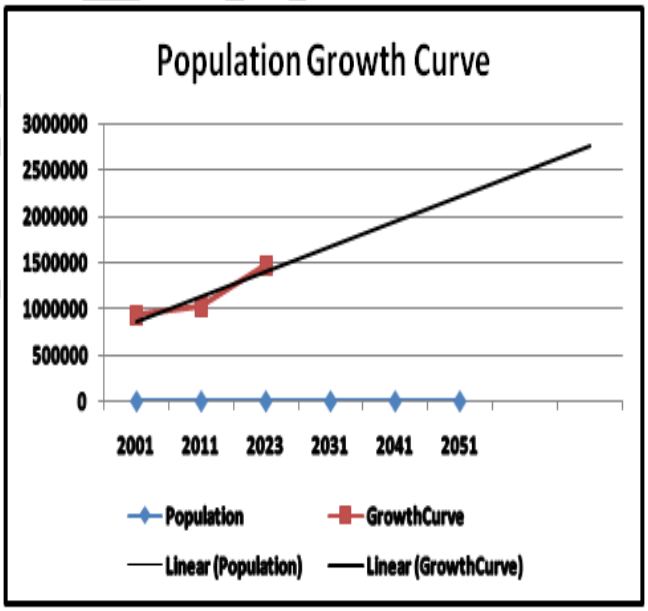

Table 1 Landuse Landcover analysis

S.No.	Classified_	1990	1990	2000	2000	2010	2010	2020	2020
	Area in Hectare	June	%	June	%	June	%	June	%
1	Water spread	209.16	1.35	128.07	0.83	373.95	2.42	657.72	4.26
2	Dense vegetation	6550.56	42.42	5453.82	35.32	4842.36	31.36	3978.09	25.76
3	Sparse Vegetation	4283.55	27.74	4707.54	30.48	3078.54	19.94	1712.25	11.09
4	Low DensityBuildup	739.26	4.79	815.49	5.28	1567.71	10.15	2526.66	16.36
5	Airport	60.03	0.39	60.12	0.39	71.01	0.46	71.01	0.46
6	High Density Buildup	948.24	6.14	1211.67	7.85	1963.62	12.72	2381.13	15.42
7	Medium Density Buildup	1365.21	8.84	1594.08	10.32	2636.55	17.07	3376.35	21.86
8	Barren Land	1078.02	6.98	1256.31	8.14	689.04	4.46	491.13	3.18
9	Rocky Exposure	173.88	1.13	178.92	1.16	148.41	0.96	148.41	0.96
10	Sandy Exposure	34.65	0.22	36.54	0.24	71.37	0.46	99.81	0.65
	Total	**15442.56**	**100.00**	**15442.56**	**100.00**	**15442.56**	**100.00**	15442.56	100

Figure 4 Landuse Landcover variation from 1990 to 2020 and future linear trend line till 2040

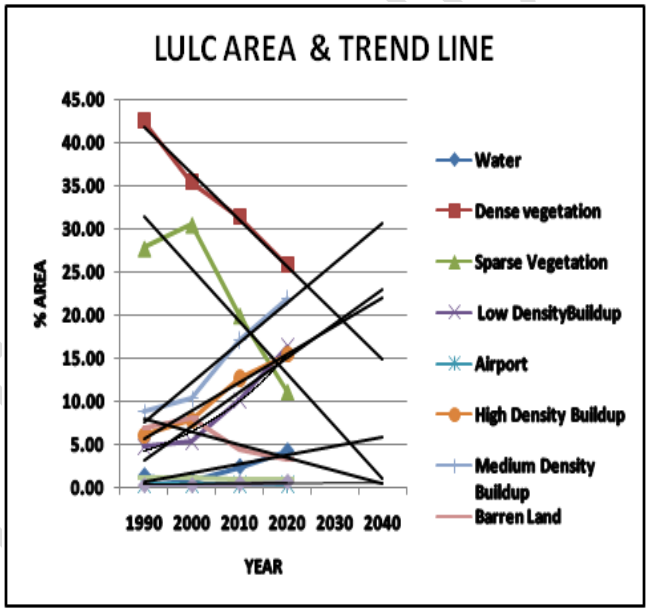

Figure 5 Landuse Landcover for the year 1990

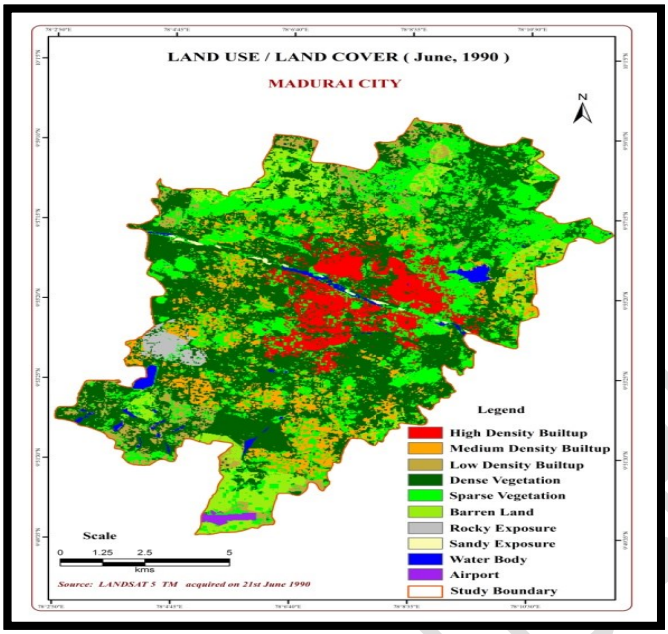

Figure 6 Landuse Landcover for the year 2000

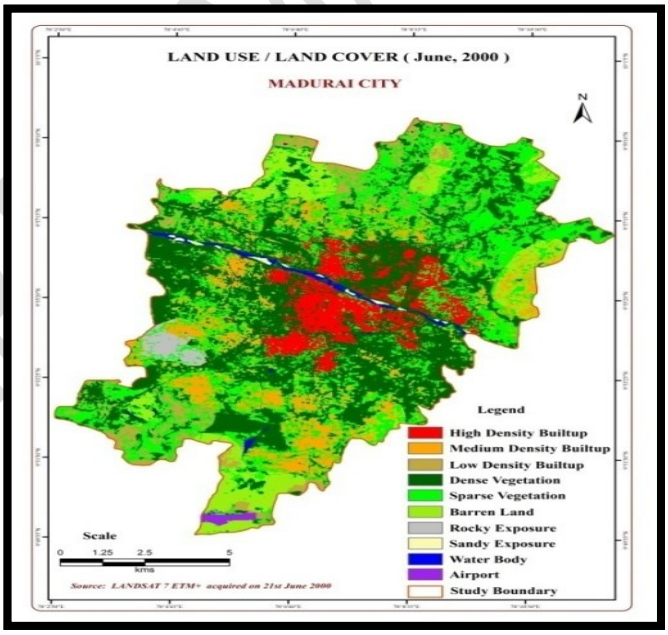

Figure 7 Landuse Landcover for the year 2010

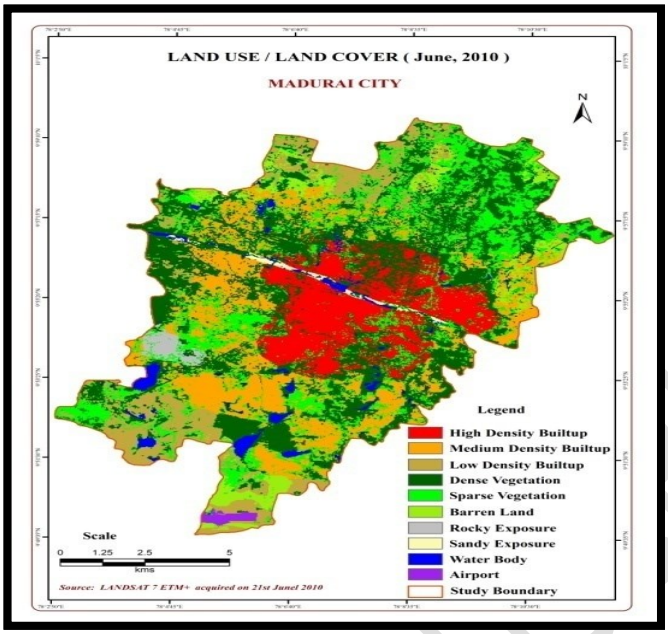

Figure 8 Landuse Landcover for the year 2020

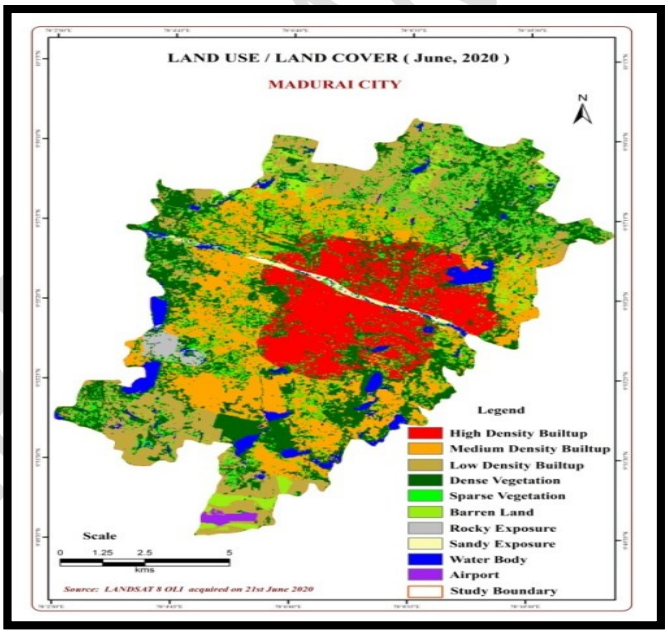

Table 2 Descriptive Statistics of Rainfall from the year 1991 to 2021

Descriptive Statistics												
	N	Range	Minimum	Maxi-mum	Sum	Mean	Mean Std. Error	Std. Deviation	Variance	Skewness	Skewness Standard Error	Kurtosis
January	31.00	87.00	22.00	109.00	1556.00	50.19	3.66	20.37	414.89	0.97	0.42	0.85
February	31.00	97.00	27.00	124.00	2025.00	65.32	4.07	22.64	512.56	0.36	0.42	-0.12
March	31.00	101.00	14.00	115.00	1647.00	53.13	3.68	20.48	419.25	0.70	0.42	1.51
April	31.00	42.00	21.00	63.00	1166.00	37.61	2.05	11.43	130.65	0.64	0.42	-0.43
May	31.00	38.00	27.00	65.00	1399.00	45.13	1.34	7.46	55.72	0.62	0.42	1.82
June	31.00	130.00	40.00	170.00	2768.00	89.29	5.75	32.01	1024.75	0.71	0.42	-0.14
July	31.00	239.00	108.00	347.00	6684.00	215.61	11.24	62.56	3914.38	0.38	0.42	-0.52
August	31.00	281.00	84.00	365.00	6418.00	207.03	12.22	68.02	4626.70	0.31	0.42	-0.17
September	31.00	127.00	23.00	150.00	2003.00	64.61	5.87	32.67	1067.05	0.51	0.42	-0.24
October	31.00	42.00	7.00	49.00	570.00	18.39	1.61	8.97	80.45	1.44	0.42	3.17
November	31.00	38.00	2.00	40.00	421.00	13.58	1.36	7.57	57.32	1.44	0.42	3.66
December	31.00	36.00	3.00	39.00	548.00	17.68	1.85	10.28	105.76	0.53	0.42	-0.77
YearlyRain	31.00	298.00	709.00	1007.00	27205.00	877.58	15.51	86.34	7454.65	-0.39	0.42	-0.91

Figure 9 Annual rainfall and Trend line from 1991 to 2021

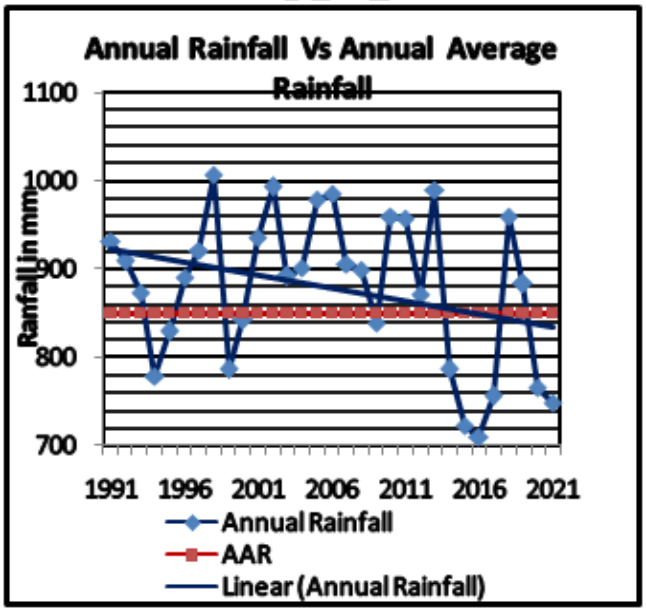

Figure 10 Yearly rainfall of a month from 1991-2021

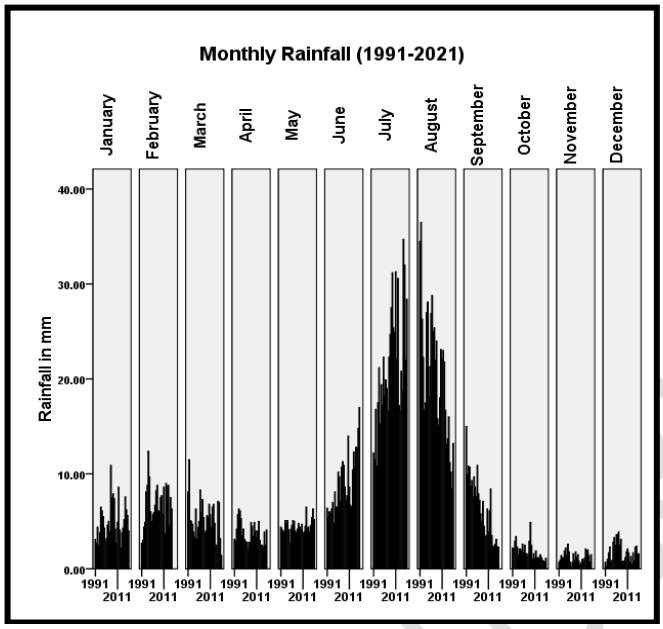

Figure 11 Average Monthly rainfall

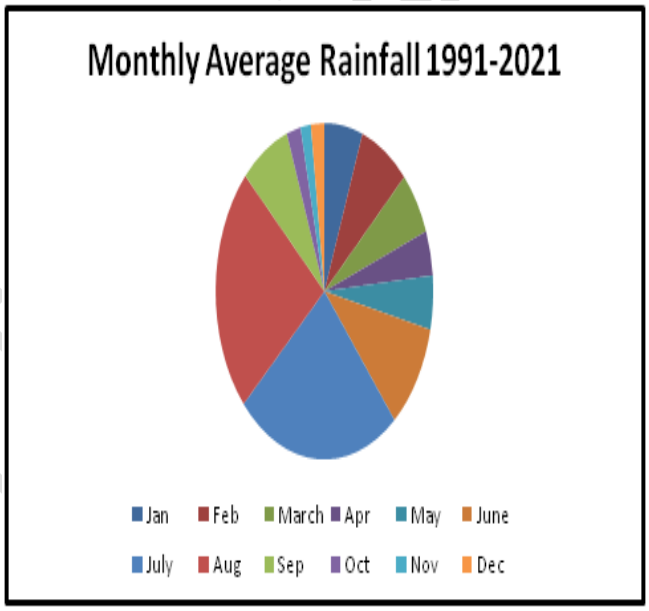

Figure 12 Yearly rainfall and Trend line for months Jan-Mar

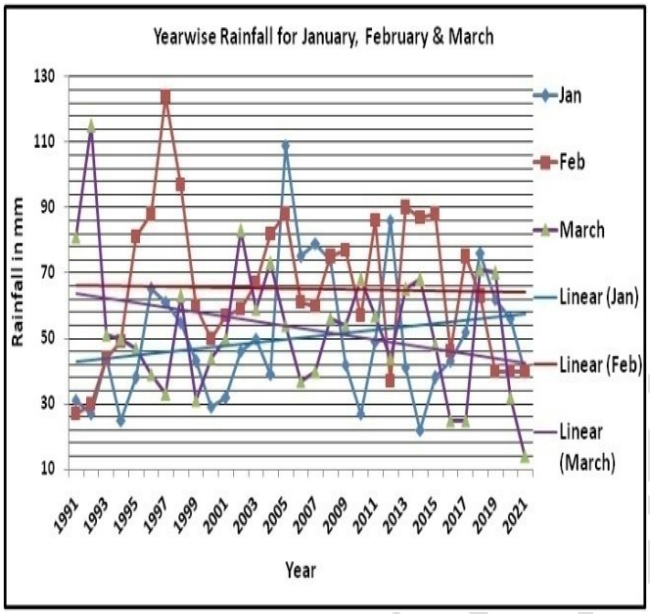

Figure 13 Yearly rainfall and Trend line for months Apr-Jun

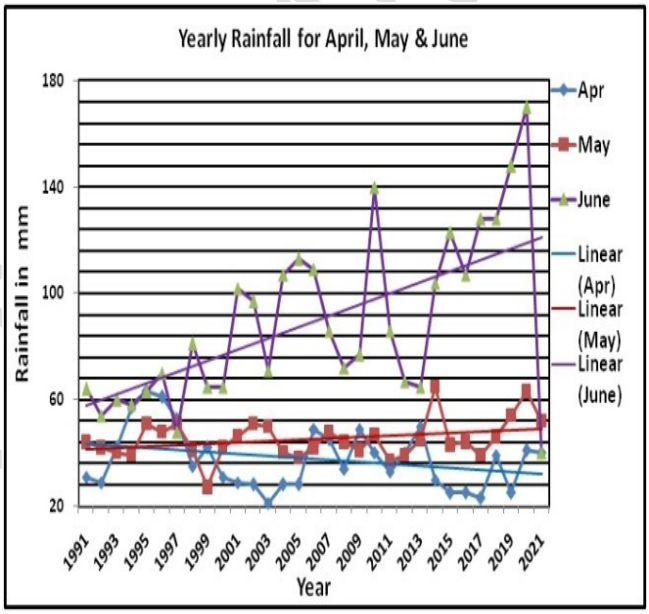

Figure 14 Yearly rainfall and Trend line for months July-Sep

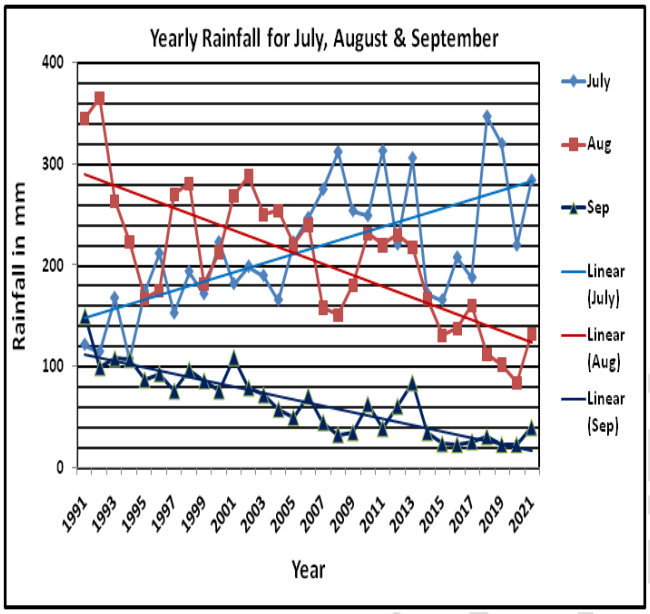

Figure 15 Yearly rainfall and Trend line for Oct-Dec

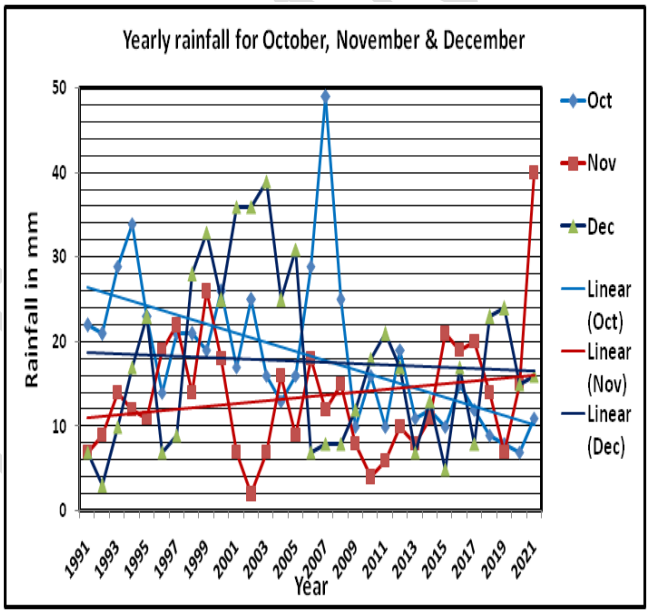

Table 3. Pearson Correlation matrix

	YearlyRainfall	January	February	March	April	May	June	July	August	September	October	November	December
YearlyRainfall	**1.00**	**0.33**	**0.22**	**0.53**	**0.06**	**-0.12**	**-0.05**	**0.26**	**0.55**	**0.38**	**0.18**	**-0.55**	**0.20**
January		**1.00**	**0.18**	**-0.23**	**0.06**	**-0.12**	**0.18**	**0.45**	**-0.24**	**-0.32**	**0.10**	**0.02**	**0.03**
February			**1.00**	**-0.13**	**0.21**	**0.00**	**-0.05**	**0.06**	**-0.05**	**-0.15**	**-0.16**	**0.06**	**0.00**
March				**1.00**	**-0.28**	**0.04**	**0.02**	**-0.13**	**0.55**	**0.31**	**-0.02**	**-0.68**	**0.06**
April					**1.00**	**0.02**	**-0.38**	**0.02**	**-0.08**	**0.29**	**0.29**	**0.15**	**-0.31**
May						**1.00**	**0.30**	**0.11**	**-0.31**	**-0.26**	**-0.19**	**-0.08**	**-0.08**
June							**1.00**	**0.28**	**-0.46**	**-0.57**	**-0.40**	**-0.23**	**0.12**
July								**1.00**	**-0.54**	**-0.57**	**-0.24**	**-0.01**	**0.02**
August									**1.00**	**0.78**	**0.33**	**-0.38**	**0.07**
September			**S**							**1.00**	**0.42**	**-0.21**	**0.07**
October											**1.00**	**-0.08**	**-0.11**
November												**1.00**	**-0.22**
December													**1.00**

Figure 16 Normal P-P chart for July

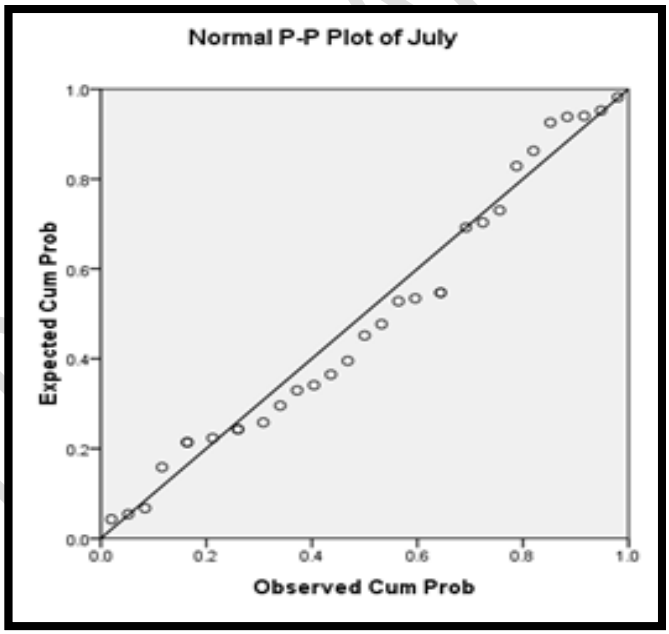

Figure 17 Detrended normal P-P chart for July

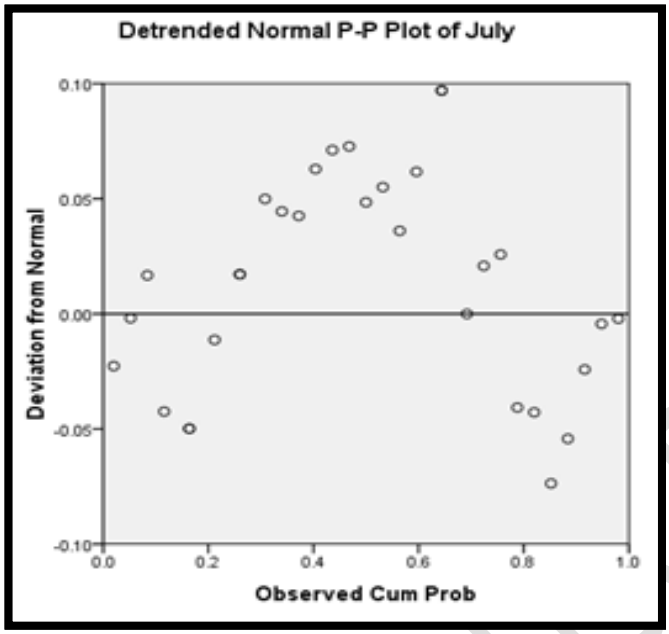

Figure 18 Normal P-P chart for the month of August

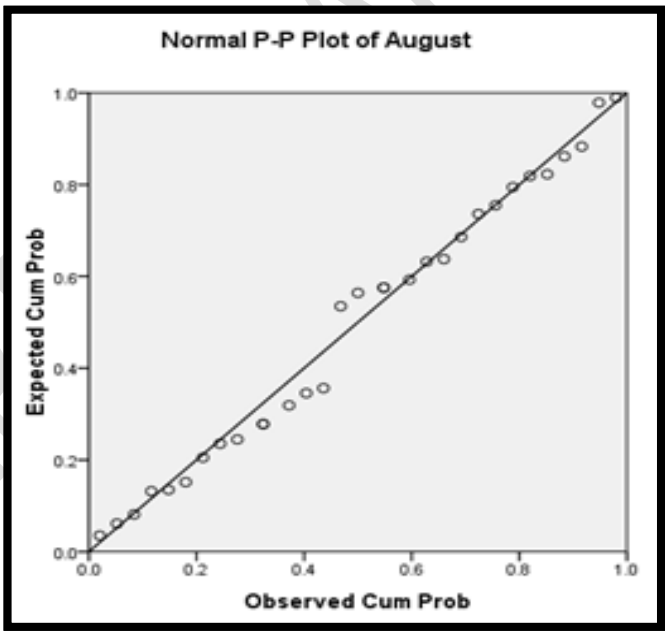

Figure 19 Detrended normal P-P chart for August

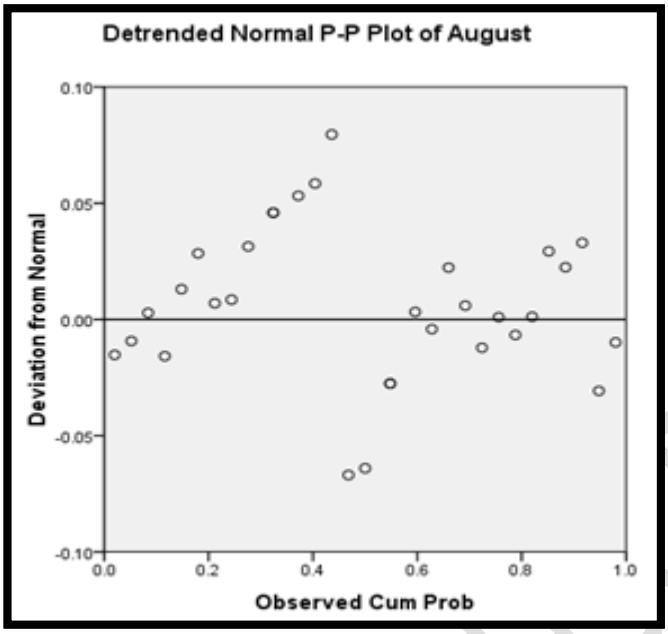

Figure 20 Box plot for monthly rainfall

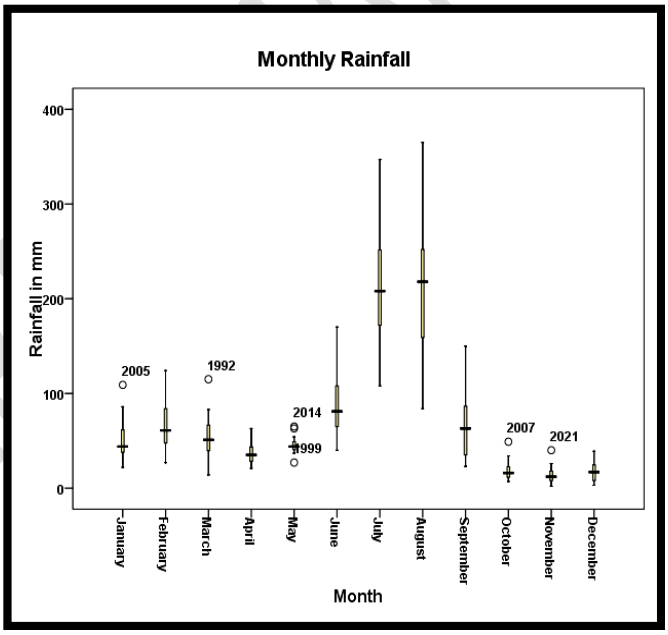

Table 4 Linear regression for annual rainfall

Month	Standardized Coefficients Beta	Month	Standardized Coefficients Beta	Month	Standardized Coefficients Beta
January	0.24	May	0.09	September	0.38
February	0.26	June	0.37	October	0.10
March	0.24	July	0.72	November	0.09
April	0.13	August	0.79	December	0.12

Figure 21 Yearly SPI Index

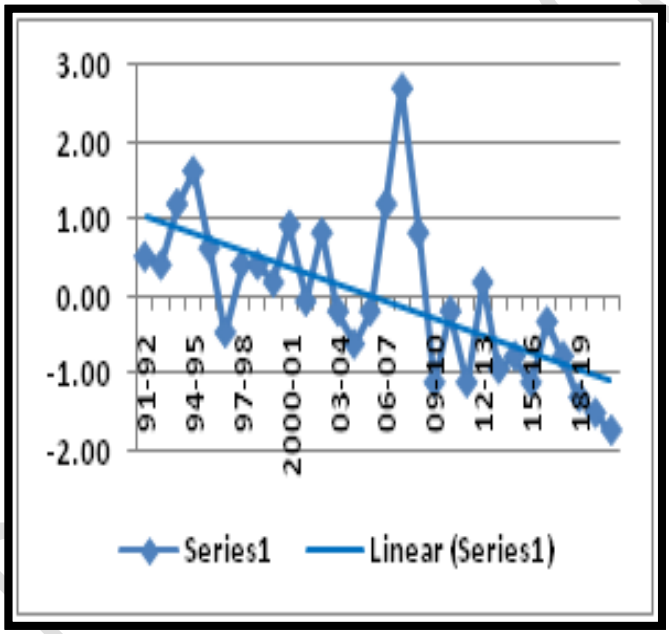

Figure 22 Monthly SPI Index for the month ofJan to March

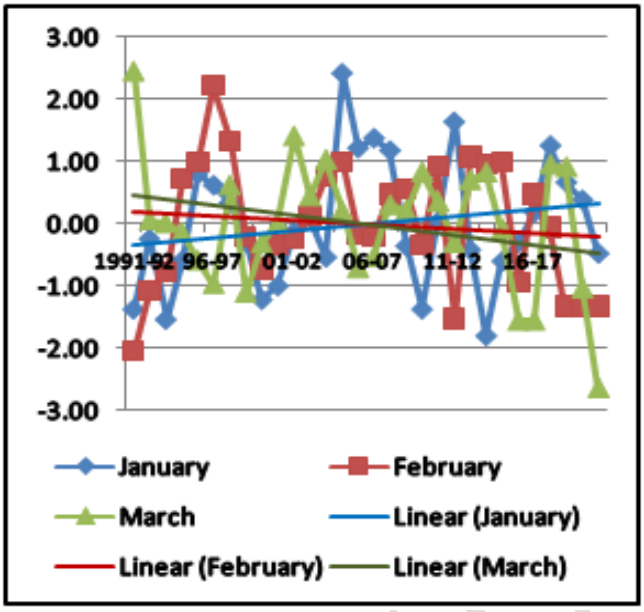

Figure 23 Monthly SPI Index for the month of April to June

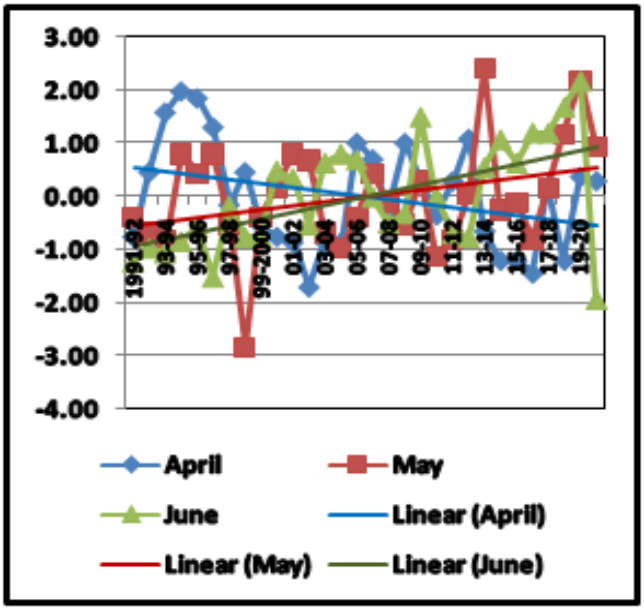

Figure 24 Monthly SPI Index for the month of July to September

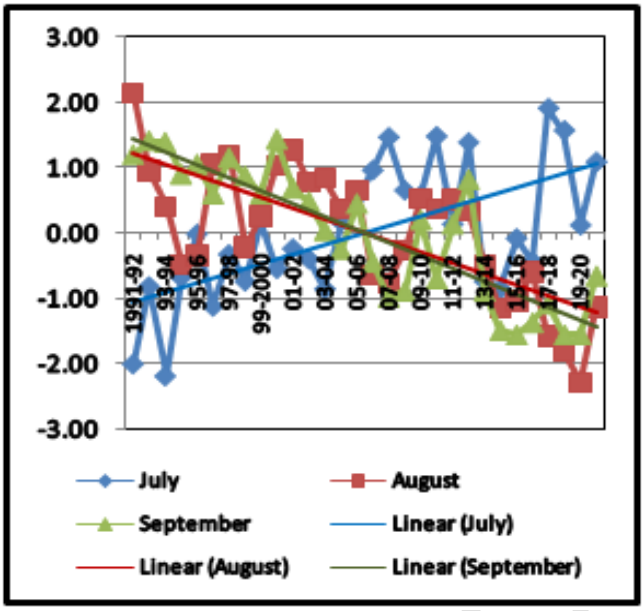

Figure 25 Monthly SPI Index for October to December

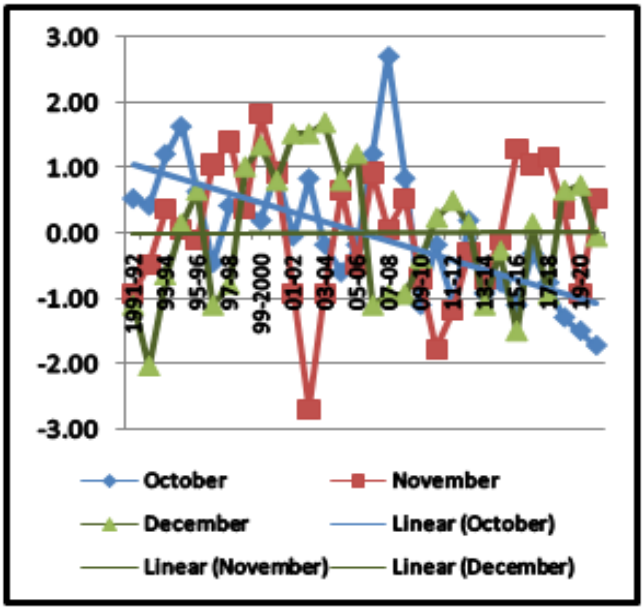

Figure 26 Yearly Maximum, Average and Minimum Temperature

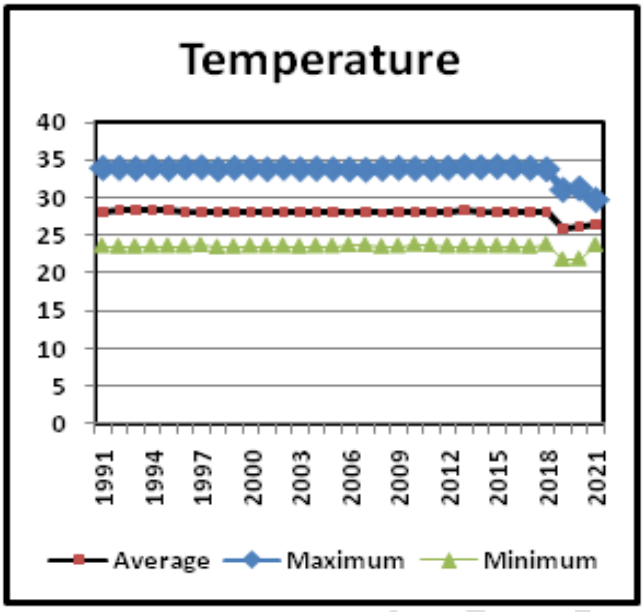

Figure 27 Land Surface Temperature of Madurai city

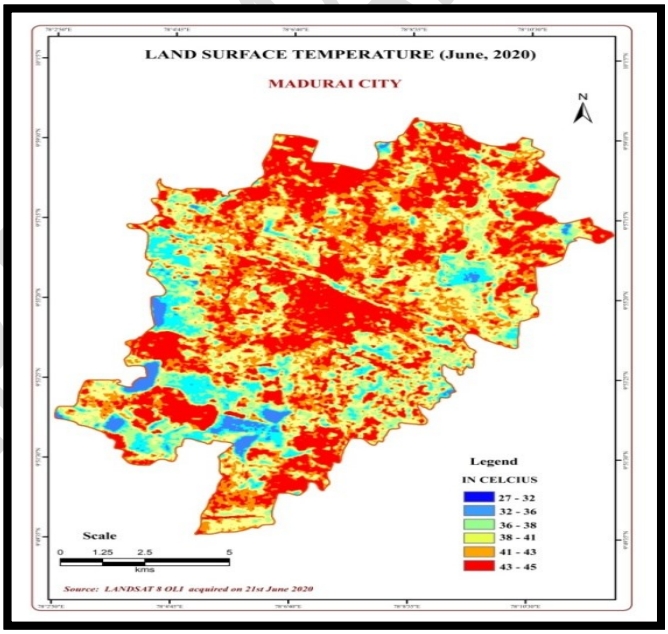

Figure 28 Google imagery of urban forestry

Figure 29 NDVI of areas of SRRC with adjoining areas

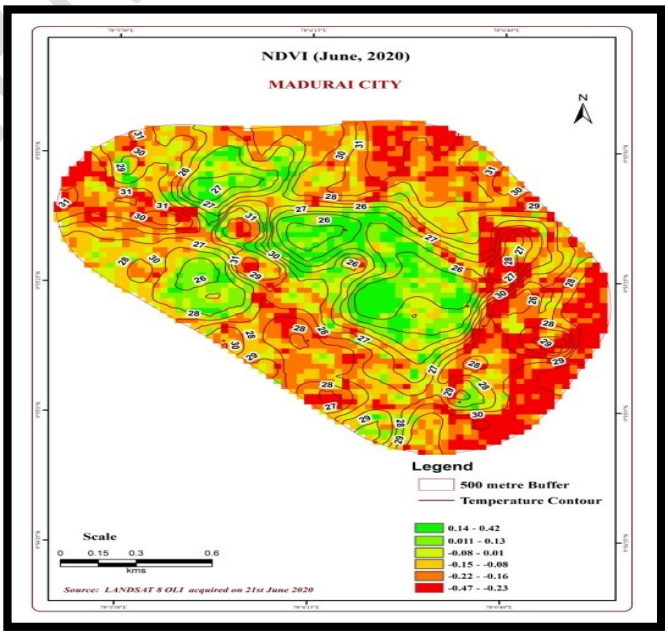

Figure 30 Map of NDVI of Madurai city

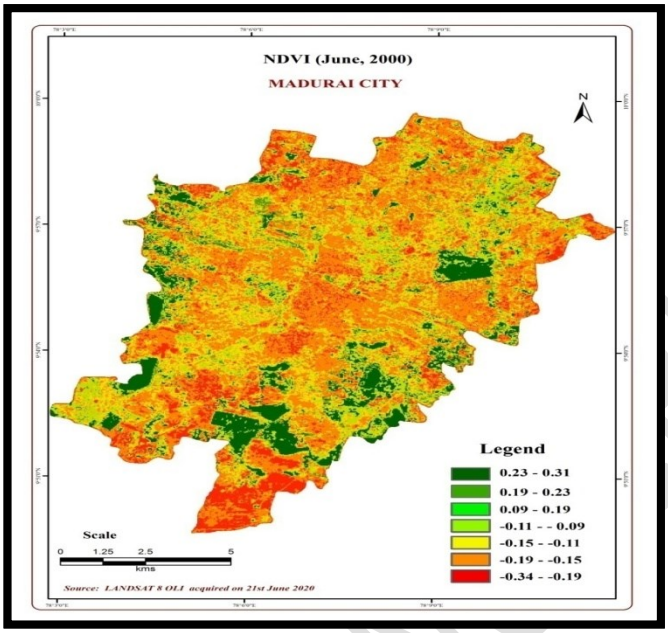

REFERENCES

Ashofteh P-S, Bozorg-Haddad O, Mariño MA (2014) Discussion of "estimating the effects of climatic variability and human activities on streamflow in the Hutuo River Basin, China". J Hydrol Eng 19(4):836–836.

Batta, B. Analysis of Urban Growth and Sprawl from Remote Sensing Data. Springer-Verlag Berlin Heidelberg, 2010.

Batty, Michael. "Geopatial analysis and modelling of urban structure and dynamics." The Geojournal, 1999.

Coombes, P. J., D. Boubli and J. Argue, Integrated Water Cycle Management at the Heritage Mews Development in Western Sydney. Presented at the 28th International Hydrology and Water resources Symposium, The Institution of Engineers, Australia, Wollongong, NSW, Australia, 10-14 November 2003.

Daniel Yeh, Pacia Hernandez, Thomas Burke, Paul Stanek, Ken Stidham, Rae Mackay, Ellen Spencer (2005), Integrated urban water management in Dunedin, Florida. United States Global Change Research Program. (n.d.). Coasts. Retrieved 12 20,2010.

Mundetia N., Sharma D., Analysis Of Rainfall And Drought In Rajasthan State, India, Global NEST Journal, Vol 17, No 1, pp 12-21, 2015.

Dr.Carlos E. M. Tucci, (2009).Integrated Urban Water Management in Jakarta. World Bank- Water Week.

George Akosa, Richard Franceys,Peter Barker and Tom Weyman-Jones (1995) "Efficiency Of Water-Supply And Sanitation Projects In Ghana" American Society of Civil Engineers1995.1:56-65.

IPCC-TGCIA (1999) Guidelines on the use of scenario data for climate impact and adaptation assessment. Version 1. Prepared by Carter, T. R., Hulme, M. and Lal, M. Intergovernmental Panel on Climate Change. Task Group on Scenarios for Climate Impact Assessment.

J.O. Odhiambo, E. Martinsson, S. Soren, P. Mboya, J. Onyango (2009) “Integration water, energy and sanitation solution for stand-alone settlements” Journal of desalination 248 (2009) 570–577.

Lairenjam C., Hodam S., Bandyopadhyay A., and Bhadra A., Historical and Temporal Trends of Climatic Parameters in North East India Global NEST Journal, Vol 19, No 4, pp 547-561.

Laura E. HigaEdaa, Weiqi Chen (2010) “Integrated Water Resources Management in Peru” Journal of Environmental Science. 2 (2010) 340–348.

Maheepala, S. and J. Blackmore, J., Integrated Urban Water Management for Cities. In Transition: Pathways Towards Sustainable Urban Development in Australia. Edited by P.W. Newton. pp. 461-478. Published by CSIRO Publishing, 2008.

Maheepala, S., J. Blackmore, C. Diaper, M. Moglia, A. Sharma and S. Kenway, Manual for Adopting Integrated Urban Water Management for Planning, Water Research Foundation (Project 4008), 6666 West Quincy Avenue, Denver, CO 80235-3098, 2010.

Mubea, Kenneth. W. "Monitoring Land-Use Change in Nakuru (Kenya) Using Multi-Sensor Satellite Data." Advances in Remote Sensing., 2012: 1,74-84.

Mundia, Charles. Ndegwa, and Aniya. M. "Analysis of Land Use Land Cover Changes and Urban Expansion of Nairobi City Using Remoote Sensing." International Journal of Remote Sensing, 2005: 2831-2849.

Nasrin SALEHNIA, Amin ALIZADEH, Hossein SANAEINEJAD, Mohammad BANNAYAN, Azar ZARRIN, Gerrit HOOGENBOOM, “Estimation of meteorological drought indices based on AgMERRA precipitation data and station-observed precipitation data”, J Arid Land (2017) 9(6): 797–809.

Pham, H.M., and Y. Yamaguch. "Urban growth and change analysis using remote sensing and spatial metrics fom 1975 to 2003 for Hanoi, Vietnam." International journal of remote sensing, 32(7), 2011: 1901-1915.

Ravindra, K.V. "Application of remote sensing and GIS technique for efficient urban planning in India." 2008.

Raskin P, Hansen E, Stavisky D, Zhu Z (1992) Simulation of water supply and demand in the Aral sea region. Water Int 17(2):55–67

Sarkar A., Impact of climate change poses a high threat to the water resources of the globe, Global NEST Journal, Vol 17, No 2, pp 323-333, 2015.

SWITCH Visioning Briefing Note: Developments in Integrated Urban Water Management (IUWM). SWITCH. (n.d.). News. Retrieved 12 15, 2010, from SWITCH Managing Water for the City ofthe Future: http://www.switchurbanwater.eu/news.php

Suresh Chand Rai, (2011), Water Management for a Megacity: National Capital Territory of Delhi. Water Resource Management, Vol. 25: 2267–2278.

Suresh Chand Aggarwal and Surender Kumar (2011) “Industrial Water Demand in India Challenges and Implications for Water Pricing. India infrastructure report.

Sokolov, A. A. and T. G. Chapman (1974), "Methods for Water Balance Computations", The UNESCO Press, Paris.

Taormina R, Chau K-W (2015) Data-driven input variable selection for rainfall-runoff modeling using binary-coded particle swarm optimization and extreme learning machines. J Hydrol 529(3):1617–1632.

Jeykumar R K C, and Chandran S (2019), Impact of urbanization on climate change and geographical analysis of physical Landuse and Landcover variation using RS-GIS, Global Nest Journal, vol. 21(03), pp. 141-152.

Kok Weng Tan et. al., (2023), Assessment Of Rainfall Pattern And Future Change For Kelantan River Basin, Malaysia Using Statistically Downscaled Local Climate Models, Global Nest Journal, vol. 25(07), pp. 139-146.

Akshaya K.G., Sathyanarayan Sridhar R (2023), Prediction of Land Use and Landcover Changes in Tiruppur Tamilnadu Using Hybrid Convolutional Neural Network, Global Nest Journal, vol. 25(06), pp. 1-11.

Withanage, W. K. N. C., Mishra, P. K., Jayasinghe B.C.(2024), An Assessment of Spatio-temporal Land Use/Land Cover Dynamics Using Landsat Time Series Data (2008-2022) in Kuliyapitiya West Divisional Secretariat Division in Kurunagala District, Sri Lanka, Journal of Geo-spatial Surveying, Vol.4(1), pp.12-23.

Kevin S. Sambieni, et. al.(2024), Climate and Land Use/Land Cover Changes within the Sota Catchment (Benin, West Africa), Vol.11(3), https://doi.org/10.3390/hydrology11030030.